

IMPROVEMENT OF THE PRESS-FORMABILITY OF ALUMINIUM SHEETS THROUGH THE CONTROL OF ANNEALING CONDITIONS

SALAH OWIES*, AKIO AOYAMA**
HIROYUKI SAIKI, NOZOMU KAWAI

Department of Mechanical Engineering

(Received Oct., 1974)

Abstract

1050-Aluminium sheets cold-rolled to 95% reduction reaching a nominal final thickness of 0.60mm. are annealed according to two annealing programmes. In the 1st, specimens are annealed for one hour at different annealing temperatures; while in the 2nd, specimens are annealed at various temperatures for different annealing intervals. The tensile properties, surface and mid-thickness textures, microscopic structure through thickness, and press-formability of sheets annealed according to the 1st programme are carefully examined. The r_{45} - and \bar{r} -values show high peak values for the partially recrystallized sheet. The n -value reaches a relatively large value and remains constant after full recrystallization. The variation of \bar{r} -value is qualitatively correlated with the texture. The development of surface and mid-thickness textures of the (112) $[11\bar{1}]$ and (123) $[21\bar{1}]$ types are recommended for high r -values. The drawability with a flat-headed punch correlates well with \bar{r} -value; while that with a round-headed one and the stretchability correlate well with the \bar{n} - and the total natural strain $\bar{\epsilon}_t$ respectively.

1. Introduction

The research on press-formability of sheet metal has made notable progress recently enhanced by the need of the industrial requirements of better understanding of sheet metal formability. The assessment of the optimum press-formability through the control of the processing variables, is based on the correlation between the press-formability of a sheet metal and its metallurgical properties as well as its tensile properties.

For steel sheets, the correlation among press-formability, metallurgical properties, and tensile properties has been well studied attaining a great extent of success¹⁾²⁾⁴⁾⁵⁾⁶⁾⁷⁾⁸⁾. This in turn led to a remarkable success in improving the drawability through the control of the processing variables¹⁾²⁾³⁾.

For aluminium sheets, the correlation among the tensile properties, the press-formability, and the processing variables have not been well established yet. The limited published data for aluminium indicate a rather small connection between the r -value and press-formability⁹⁾¹⁰⁾¹¹⁾. Wright¹²⁾ found that good press-formability

* Assiut Univ., Egypt.

** Nihon Densō Co. Ltd.

can be associated with high r -values. Gokyu *et al.*¹³⁾ suggested a correlation between the press-formability and the r_{45} -value (the tension axis is at 45° to the rolling direction). Kawai *et al.*⁹⁾ reported that the drawability correlates well with the minimum value of r among the 0°, 45°, and 90° directions to the rolling direction in the plane of the sheet, when a flat-headed punch was used. With a round-headed punch, the drawability of the as-cold rolled sheets correlates well with the n -value obtained by the bulge test, and that of the annealed sheets correlates well with the n -value obtained by the tensile test. Rogers and Anderson¹⁰⁾ maintained that when the deformation was primary stretching, best drawability was obtained with high r - and high n -values. OKi *et al.*¹⁴⁾ suggested that the deep-drawability (evaluated by a single blank test) increases with the \bar{r} -value*. Riggs¹¹⁾ reported a fair correlation between the r_0 -value and the drawability, while a weak one was found for \bar{r} -value.

With respect to the processing variables, Gokyu *et al.*¹⁵⁾ suggested an optimum soaking temperature in the range from 500°C to 560°C for 2 hours to improve the drawability of aluminium, which has been also shown to increase with an increasing cold-reduction prior to annealing. Grimes *et al.*¹⁶⁾ reported that better drawability was attained for a sheet 20% cold-rolled, and that the best drawability was gained for a heavily cold-rolled sheet (up to 90%) annealed to maximum recovery without recrystallization. Kawai *et al.*¹⁷⁾ suggested that the best drawability was obtained for a heavily cold-rolled sheet partially recrystallized. However, the properties of sheets cold-rolled to more than 90% have not been examined yet, inspite of the possibility of improving the press-formability. Also, it was suggested by Kamijo *et al.*³³⁾³⁴⁾ that friction in cold-rolling unexpectedly influenced the properties of the annealed sheet.

Considering the above mentioned situation of aluminium sheets, a more comprehensive investigation is needed to better reveal the correlation among the tensile properties, the texture, and the press-formability. The present work is undertaken to meet this need and to find the optimum processing conditions for the sake of improving the press-formability, focusing on the processing variables mentioned above, i. e., cold-reduction and friction in cold-rolling, and the final annealing process. In this paper, the various properties of the 95% cold-rolled sheet are examined in detail.

2. Experimental Analysis

2. 1. Material:

The material used is high-purity aluminium [JIS H 4000 A 1050 P-R] the chemical composition and mechanical properties of which are given in table 1-(a) & (b).

Table 1-(a) Chemical composition (wt. %), JIS H 4000 A 1050 P-R.

	Cu	Si	Fe	Mn	Mg	Zn	Ti	Al
allowable	≤0.05	≤0.25	≤0.40	≤0.05	≤0.05	≤0.05	≤0.03	≥99.50
tested	<0.01	0.10	0.32	<0.01	<0.01	<0.01	0.01	99.61

* $\bar{r} = (r_0 + 2r_{45} + r_{90})/4$

Table 1-(b) Mechanical Properties.

	σ_u kg/mm ²	total elong. %	r-values of supplied sheets, annealed: 350°C X 1 hr.			
allowable	≥ 7	≥ 16	r_0	r_{45}	r_{90}	\bar{r}
tested	8	54	0.40	0.90	0.38	0.645

2. 2. Processing sequences and conditions of material:

The processing sequences are shown in fig. 1. The cold rolling conditions and mill specifications are given in table 2-(a) & (b). The final annealing of the test specimens was carried out in a salt bath to within $\pm 1^\circ\text{C}$.

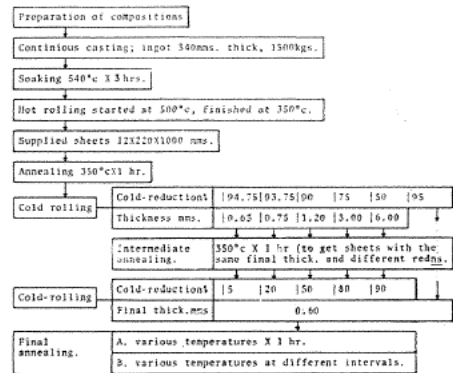


Fig. 1. Processing of aluminium sheets.

Table 2-(a) Rolling conditions.

Type of rolling	unidirectional; sheets are passed through the rolls in the same direction.
Lubricant: applied to both rolls and sheet.	mineral oil + oleic acid 1%, viscosity: 11.96cSt/100°F, coeff. of friction: 0.122
Total number of passes	27 to reach a nominal final thickness of 0.60mm.
Reduction per pass	about 15%

Table 2-(b) Mill specifications.

Working rolls	80φ×250 mms.	Rolling speed	35m/min.
Supporting rolls*	300φ×250	Thickness control	right & left screwdowns operated at the same time.
Roll material	high C & high Cr steel.		
Roll surface hardness	$R_c > 85$	Motor output	45 kw.

* Surface roughness: $R_{\max} \leq 2\mu\text{m}$.

2. 3. Tensile test:

Tensile test specimens of ISO-type were cut off at 0° , 45° , and 90° to the rolling direction in the plane of the sheet, fig. 2. For softer specimens (natural strain $\epsilon_t > 0.15$), the plastic strain ratio r is calculated from ϵ_b/ϵ_t , the width strain ϵ_b is measured while the thickness strain ϵ_t is calculated applying the volume constancy law. For harder specimens, ϵ_b and ϵ_t are measured at 13 points and 13 X 3 points of intersection of a previously scribed grid pattern on the specimen surface respectively (measurements are made on fractured specimens). For these specimens, r -values are calculated only from specimens showing approximately equal strains at the uniformly deformed regions on both sides of the neck. A representative r -value is the average of the r -values at these uniformly deformed regions. For harder specimens, the work-hardening index n is substituted by ϵ_t at the maximum tensile load. While for softer specimens, it is estimated from the power law $\sigma = F\epsilon^n$ applied to the $\log \sigma$ - $\log \epsilon$ diagram, where σ is the true stress, ϵ is the true strain, F is the material constant.

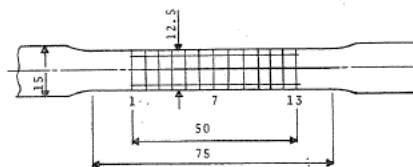


Fig. 2. Tensile-test specimen, ISO type.

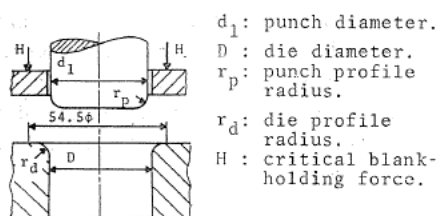


Fig. 3. Schematic representation of deep-drawing.

2. 4. Preferred orientation (texture):

Texture is specified by means of pole figures made by using a Rigaku-full automatic-Pole figure X-ray diffractometer, and applying $\text{CuK}\alpha$ radiation. The Shultz reflection method¹⁸⁾ and the Decker, Asp., and Hecker¹⁹⁾ transmission method are used, applying a correction factor for absorption for the latter and overlapping at 40° away from the centre in order to construct a complete pole figure^{20,21)}.

Specimens for texture inspection are 0.10mm. thick; they are prepared of both surface and mid-thickness of the 0.60mm. thick finished sheets. A dilute hydrofluoric acid solution is used for etching out layers of aluminium up to the required thickness; for the surface specimens the surface is protected from the acid by a layer of paraffin wax.

2. 5. Press-forming :

Deep-drawability of aluminium is evaluated by determining the limiting drawing ratio (L. D. R.), following the procedure adopted by Kawai *et al.*⁹⁾. The working conditions of the deep-drawing test are given in table 3, while fig. 3 illustrates the notations used. The stretch-formability is examined by carrying out the Erichsen and pure-stretch tests, the working conditions of which are also given in table 3. Blanks for press-forming tests are carefully prepared taking Kemmis²²⁾ recommendations into consideration.

Table 3 Working conditions of deep-drawing, pure-stretch, and Erichsen tests.

	Deep-drawing test		Pure-stretch test
Tool	Punch	$d_1=40\phi$, $r_p=6$, 20mms.	$d_1=40\phi$, hemispherical
	Die	$D=42.5\phi$, $r_d=6$ mms.	$D=42.5\phi$, $r_d=6$ mms.
Lubricant	blank-holder and die suface.	tallow(3) + gra-phite(1), by wt.
	punch surface	rosin, bees-wax	rosin, bees-wax
Punch speed	0.20 mm/sec.		0.20 mm/sec.
Blank holding	critical ($2 \times$ Siebel' s semi theoretical value 23).		screw clamping by means of beeds.
Δ	0.025, drawing ratio interval for determining L. D. R.	
Tester	Deep-drawing testing machine, model TF-102, KOKI Co. Ltd., Tokyo, Japan.		

N. B.: The Erichsen test is carried out according to JIS B7777, the tools used are according to JIS B 7729.

3. Experimental Results

3. 1. *Effect of cold-reduction on the tensile properties and press-formability:*

These properties have been investigated for sheets cold-rolled to 5%, 20%, 50%, 80%, 90%, and 95%. It was found that both the r - and n -values seem to be unaffected by cold-reduction. LDR values obtained with flat-headed punch seem to be also unaffected; while those obtained with round-headed punch decrease with the increase of cold-reduction. The Erichsen value remains approximately constant, while the pure-stretch value decreases gradually with an increasing cold-reduction.

In view of these results, it can be concluded that for the as cold-rolled sheets, the cold-reduction cannot be considered as a factor to improve the press-formability. This has been also reported by Kawai et al.⁹⁾. It was reported that an increasing cold-reduction prior to a certain annealing condition increased the r -value⁹⁾¹⁷⁾²⁴⁾. Seeking the improvement of the press-formability of aluminium sheets, the effects of annealing conditions on the properties of the 95% cold-rolled sheets are to be carefully examined.

3. 2. *Effects of annealing conditions:*

3. 2. 1. *Tensile properties of specimens annealed according to programme 'A' (various temperatures \times 1 hr.):*

Both Vicker' s hardness and ultimate tensile strength decrease rapidly with an increasing annealing temperature until reaching a constant value after full recrystallization, fig. 4. The recrystallization begins at about 250°C and ends itself at about 300°C. This can be concluded from the effect of annealing temperature on the hardness and on the tensile properties, also from the microscopic structure examination and the texture data to be mentioned later.

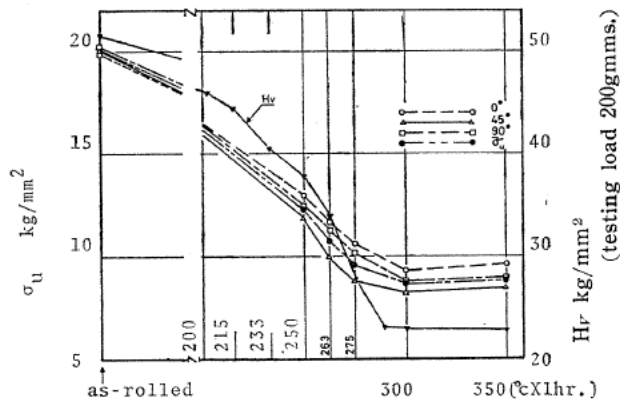


Fig. 4. Effect of annealing temperature on ultimate tensile strength & Vicker's hardness.

For the r -value the following can be noted from fig. 5:

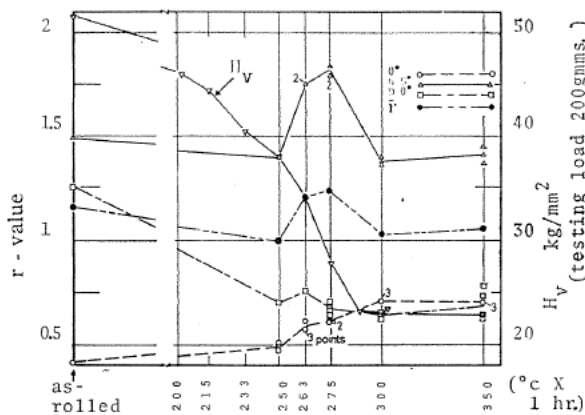


Fig. 5 Effect of annealing temperature on r -value

a) r_0 -value increases with an increasing annealing temperature showing a step increase between 250°C and 263°C, reaching a constant value after full recrystallization.

b) r_{45} -value increases suddenly at 250°C (commence of recrystallization), reaching a peak (1.83) at 275°C then it decreases and remains constant after full recrystallization. The \bar{r} -value shows the same tendency as that of r_{45} -value. The r_{45} -value is always highest among the r_0 -, r_{45} - and r_{90} -values.

c) r_{90} -value decreases with the increase of annealing temperature reaching a constant value after full recrystallization; it shows a little increase at 263°C.

The above characteristic variation of r -value is completely different from the result previously reported by Kawai *et al.*¹⁷⁾ in which the order among r -values is reversed with the commence of recrystallization.

As shown in fig. 6:

The n -value and the total natural strain ϵ_t increase rapidly as soon as raecrystallization commences, reaching a maximum constant value after full recrystallization. The differences among these values in 0° , 45° , and 90° directions are relatively small.

3.2.2. *Tensile properties of specimens annealed according to programme 'B' (various temperatures at different annealing intervals) :*

The effect of annealing time on both of the hardness and the r -value is shown in fig. 7. These values vary with an increasing annealing time in approximately the same way as they did with the annealing temperature for specimens annealed according to programme 'A'. The \bar{r} -value obtained at partial recrystallization ($350^\circ\text{C} \times 24 \text{ sec.}$),

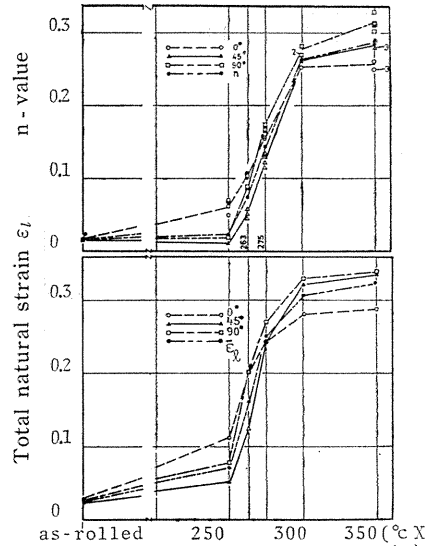


Fig. 6. Effect of annealing temperature on n -value & total natural strain.

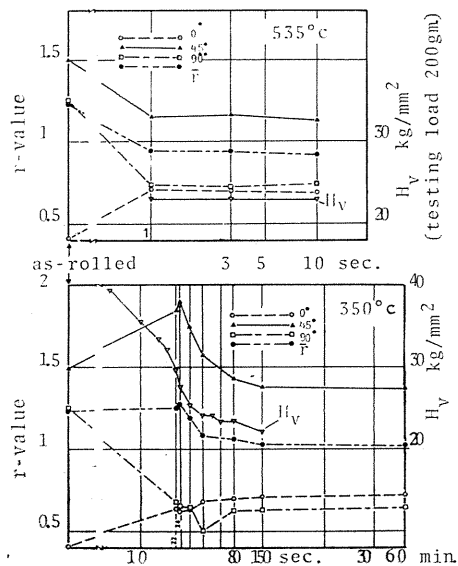


Fig. 7. Effect of annealing time on r -value.

about 1.26, is approximately equal to that of specimens ($\bar{r}=1.24$) annealed according to programme 'A' for partial recrystallization.

While the effects of annealing temperature on hardness, ultimate tensile strength, and n -value (to some extent), are understandable, the characteristic variation of r_{45} (and \bar{r}), as it affects formability- to be mentioned later- is to be clarified.

3. 3. Press-formability:

Deep-drawability: as shown in fig. 8:

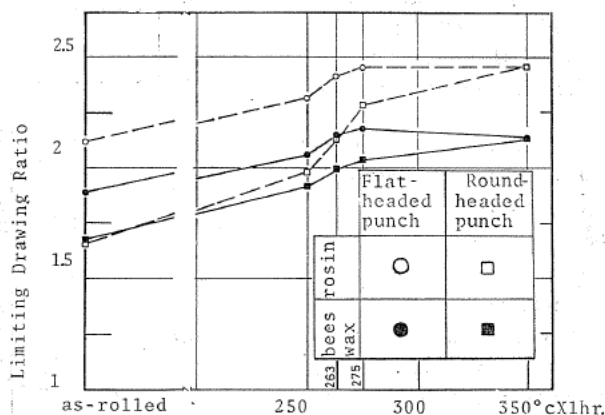


Fig. 8. Effect of annealing temperature on the limiting drawing ratio (LDR).

a) LDR values increase rapidly as recrystallization commences reaching a constant value after full recrystallization, independently of both punch profile and lubricant over punch head. At 275°C, LDR reaches a peak for the flat-headed punch.

b) When using rosin as lubricant over punch head, differences among LDR values with flat-headed and round-headed punches are larger than those obtained when using bees-wax.

c) With a flat-headed punch, the differences between LDR values obtained with rosin and bees-wax are approximately constant. While with a round-headed punch, these values are approximately equal up to 250°C, then the difference increases rapidly.

d) At full recrystallization, the specimens are equally drawable with both of the punch head types.

It can be easily observed that the result of a) corresponds to the variation of \bar{r} -value shown in fig. 5. Those of b), c), and d) reveal the effects of the punch profile and friction in connection with the metal properties, which were discussed in detail by Swift²⁵⁾ and Kawai *et al.*²⁶⁾²⁷⁾.

Stretch-formability: as shown in fig. 9:

Both of the Erichsen and pure-stretch values increase rapidly with the increase in annealing temperature up to full recrystallization where they attain a maximum and constant value. Erichsen values of specimens annealed according to programme 'B' show the same tendency with an increasing annealing time, fig. 10. Pure-stretch values are higher with bees-wax than with rosin as lubricants over punch head. The difference increases as the annealing temperature increases.

The variation of LDR values obtained with a flat-headed punch can be relatively well correlated with that of \bar{r} -value. While the variation of LDR values obtained with a round-headed punch can be rather correlated with the variation of n -value. The Erichsen and pure-stretch values mainly correlate with the variation of n -value and the total natural strain respectively²⁸⁾.

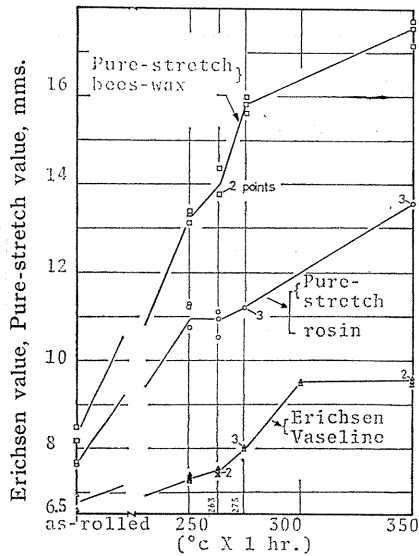


Fig. 9. Effect of annealing temperature on Erichsen & Pure-stretch values.

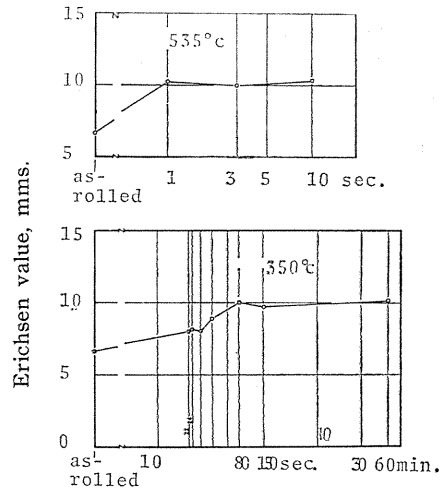


Fig. 10. Effect of annealing time on Erichsen value.

Fig. 11 shows the r -, n -, Erichsen-, and pure-stretch-values for the 90% and

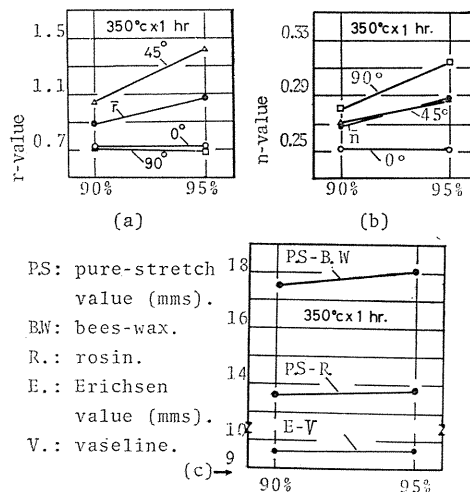


Fig. 11. r , n , Erichsen and pure-stretch values of 90% & 95% cold-rolled sheets, fully recrystallized.

95% cold-rolled specimens after full recrystallization. The \bar{r} , r_{45} , \bar{n} , n_{45} , n_{90} , and the pure stretch values are higher for the 95% than the 90% prior cold-reductions. It can be concluded that the increase of the prior cold-reduction improves r - and n -values and the stretch-formability.

Four ears are developed at 45° to the rolling direction, independent of the cold-reduction and annealing temperature; this is the maximum r -value direction.

4. Discussions

As mentioned before, the characteristic variation of r -value according to the annealing conditions is to be carefully clarified. In order to throw some light on the mechanism of the variation of r -value, microhardness, microscopic structure, and texture of sheet metal will be examined through the thickness.

A hardness distribution through the thickness of the partially annealed specimen ($275^{\circ}\text{C} \times 1 \text{ hr.}$) is shown in fig. 12. The indenter is impressed with the lightest weight 25gmms. normally to the sheet surface etched out and electropolished gradually. It is observed that the region near the surface is softer than the mid-thickness region.

Plate 1-(a) shows a microscopic structure examination through the thickness of a specimen annealed at $250^{\circ}\text{C} \times 1 \text{ hr.}$ It can be observed that recrystallized grains are hardly found. For the $263^{\circ}\text{C} \times 1 \text{ hr.}$ annealed specimen, plate 1-(b), few

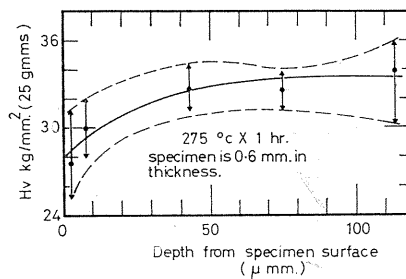
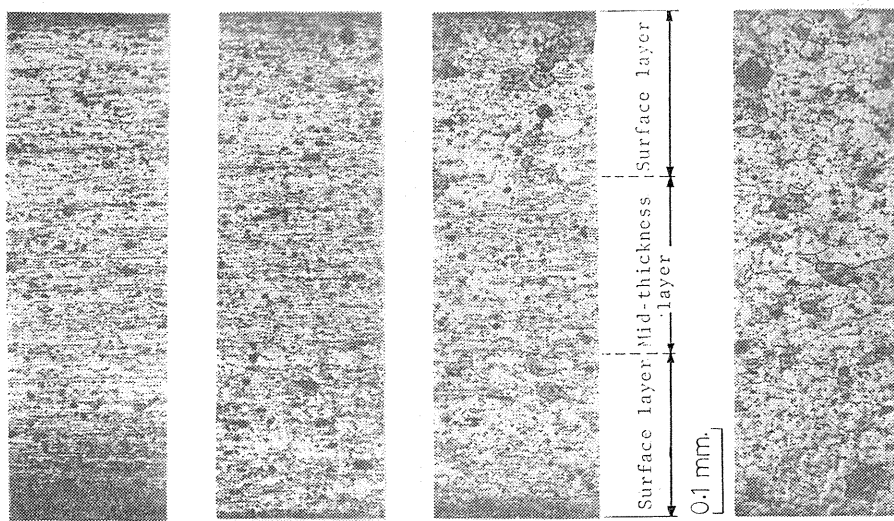


Fig. 12. Micro-hardness distribution through the thickness of the 95% cold-rolled specimen, partially recrystallized.



(a) $250^{\circ}\text{C} \times 1 \text{ hr.}$ (b) $263^{\circ}\text{C} \times 1 \text{ hr.}$ (c) $275^{\circ}\text{C} \times 1 \text{ hr.}$ (d) $350^{\circ}\text{C} \times 1 \text{ hr.}$

Plate. 1. Microscopic structure through thickness of the 95% cold-rolled sheet.

of these grains appear in the surface region. In the surface region of the $275^{\circ}\text{C} \times 1 \text{ hr.}$ annealed specimen, plate 1-(c), the recrystallized grains are so developed that a surface layer and a mid-thickness layer with most of the grains in the as-rolled condition, seem to be existing; i. e., a sandwich like structure. Plate 1-(d) shows the $350^{\circ}\text{C} \times 1 \text{ hr.}$ annealed specimen in the recrystallized state. The earlier recrystallization in the surface layer is likely due to the severe surface deformation

produced by the frictional shearing stress²⁹⁾.

Sets of $\{111\}$ and $\{200\}$ pole figures of the surface and mid-thickness layers of the as cold-rolled, partially recrystallized and fully recrystallized specimens are

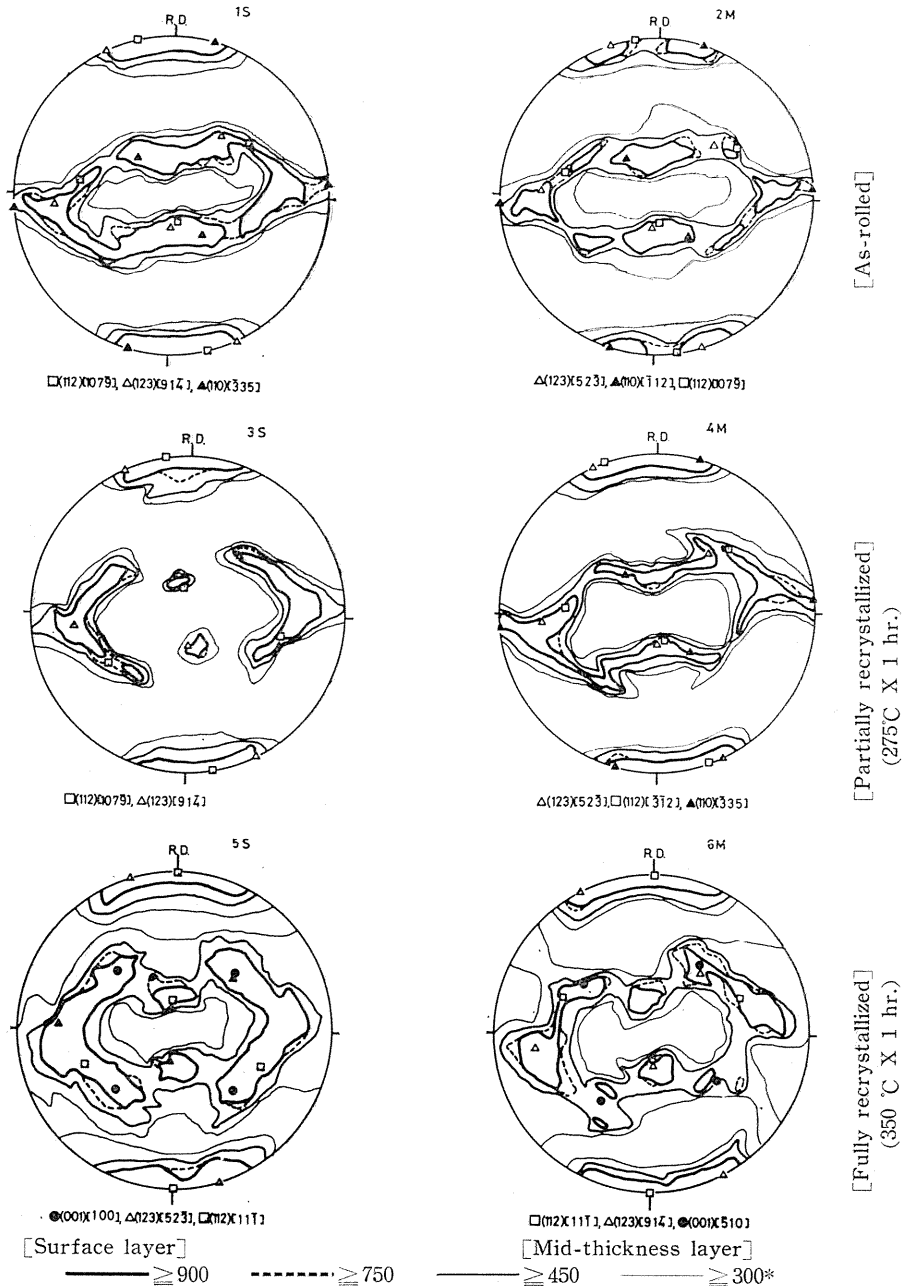


Fig. 13. $\{111\}$ Pole figures at both surface and mid-thickness layers of the 95% cold-rolled sheet.

* : Intensities in arbitrary units.

reproduced in figs. 13 and 14 respectively. Table 4 summarizes the textures developed.

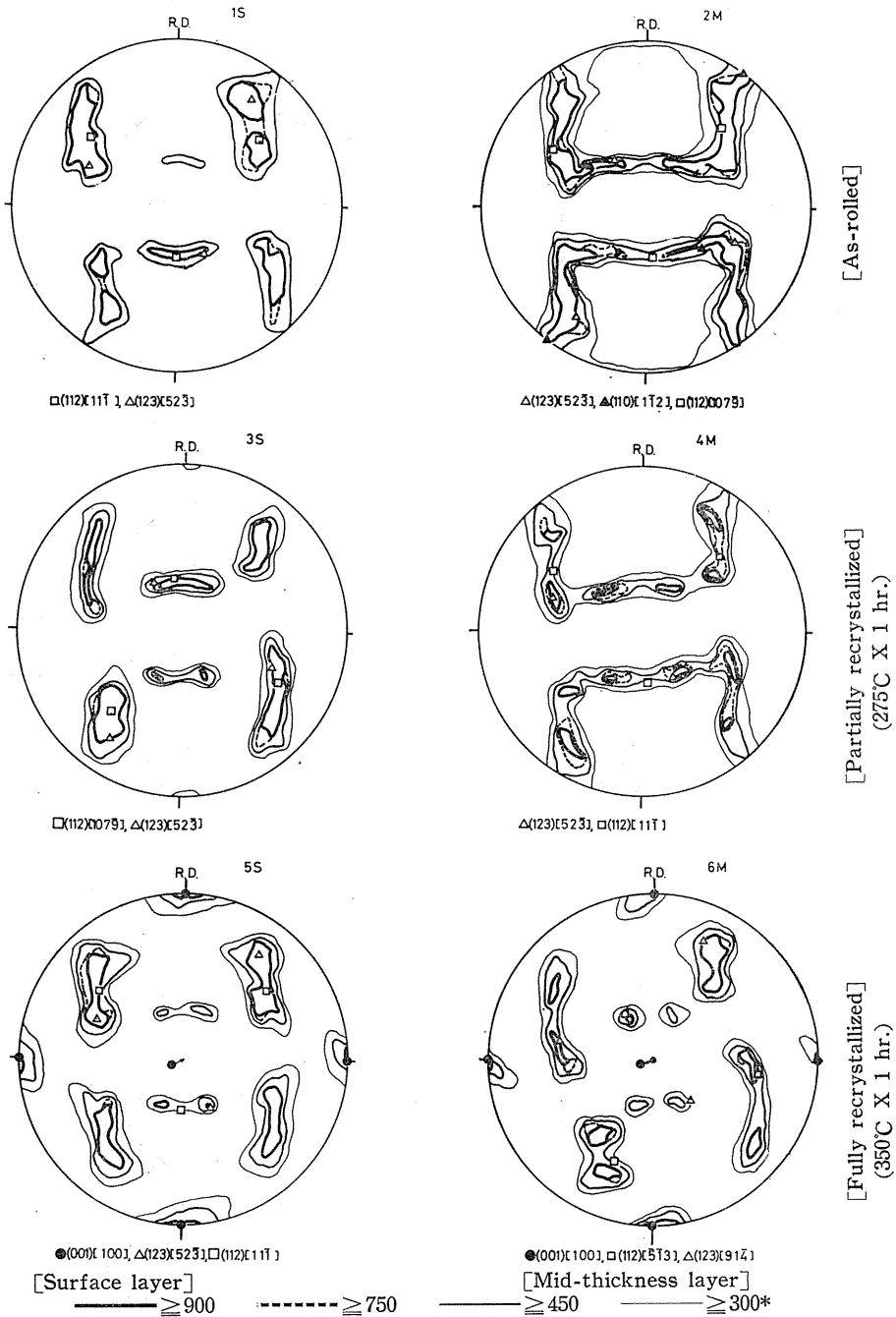


Fig. 14. {200} Pole figures at both surface and mid-thickness layers of the 95% cold-rolled sheet.

* : Intensities in arbitrary units.

Table 4 Surface and mid-thickness textures of the 95% cold-rolled sheet.

	Surface layer	Mid-thickness layer
As	1 (112) $[\bar{1}1\bar{1}]$	3 (112) $[\bar{1}1\bar{1}]$ (n. t.)
Cold-rolled.	2 (123) $[\bar{2}1\bar{1}]$ (n. t.)	1 (123) $[\bar{2}1\bar{1}]$
	3 (110) $[\bar{1}12]$ (n. t.)	2 (110) $[\bar{1}12]$
Partially recrystallized (275°C X 1 hr.).	1 (112) $[\bar{1}1\bar{1}]$ (n. t.)	2 (112) $[\bar{1}1\bar{1}]$ (n. t.)
	1' (123) $[\bar{2}1\bar{1}]$ (n. t.)	1 (123) $[\bar{2}1\bar{1}]$ (n. t.)
		4 (110) $[\bar{1}12]$ (n. t.)
Fully recrystallized (350°C X 1 hr.)	3 (112) $[\bar{1}1\bar{1}]$	2 (112) $[\bar{1}1\bar{1}]$ (n. t.)
	1' (123) $[\bar{2}1\bar{1}]$ (n. t.)	3 (123) $[\bar{2}1\bar{1}]$ (n. t.)
	1 (001) $[\bar{1}00]$	1 (001) $[\bar{1}00]$ (n. t.)

N. B.: a) (n. t.): near to.

b) numbers indicate intensity order, e. g., 1 is of highest intensity.

The presence of a sandwich-like structure can be revealed by the microhardness, the microscopic structure and texture results. For the as rolled state, the intensity of (112) $[\bar{1}1\bar{1}]$ texture of the surface layer is larger, the intensity of (123) $[\bar{2}1\bar{1}]$ is relatively lower, while that of (110) $[\bar{1}12]$ is lower compared with similar textures of the mid-thickness. In the partially recrystallized condition the (110) $[\bar{1}12]$ texture is weakened in the mid-thickness layer, and it disappears in the surface layer. The (112) $[\bar{1}1\bar{1}]$ remains approximately unchanged, but the (123) $[\bar{2}1\bar{1}]$ is strengthened in the surface layer; while (123) $[\bar{2}1\bar{1}]$ remains unchanged, (112) $[\bar{1}1\bar{1}]$ is strengthened in the mid-thickness layer. The (001) $[\bar{1}00]$ texture strongly developed in both the surface and the mid-thickness layers of the fully recrystallized state, while the (112) $[\bar{1}1\bar{1}]$ and (123) $[\bar{2}1\bar{1}]$ textures are weakened.

Similar texture results, of both the surface and mid-thickness of heavily cold-rolled aluminium sheets under low friction condition in the as-rolled and fully recrystallized states were reported⁽³⁰⁾⁽³¹⁾⁽³²⁾⁽³³⁾⁽³⁴⁾.

The results of Hosford and Backofen⁸⁾ and Gokyu et al.³⁵⁾, show that a relatively strong component of (001) $[\bar{1}00]$ texture lowers markedly the \bar{r} -value, specially the r_{45} -value relative to both r_0 - and r_{90} -values. The (110) $[\bar{1}12]$, (112) $[\bar{1}1\bar{1}]$ and (123) $[\bar{1}2\bar{1}]$ textures raise the r_{45} -value. The (112) $[\bar{1}1\bar{1}]$ texture increases sensitively the r_{45} -value, also (112) $[\bar{1}1\bar{1}]$ and (123) $[\bar{1}2\bar{1}]$ do the same for r_{90} -value. The (110) $[\bar{1}12]$ lowers the r_0 -value.

Bearing these results in mind, and referring to the present texture results mentioned above, it can be deduced that the \bar{r}_s (\bar{r} -value of surface layer) is relatively larger than \bar{r}_m (\bar{r} -value of mid-thickness layer) for the as-rolled state. Both of them increase for the partially recrystallized condition (\bar{r}_s is still larger), and are lowered markedly due to the strong presence of (001) $[\bar{1}00]$ component in the full recrystallized state. The cold-rolling in this research is carried out under relatively good lubricating condition. And as the surface texture development is controlled by the friction between the rolls and specimen surfaces²⁹⁾, the average value of both \bar{r}_s and \bar{r}_m is closer to \bar{r}_m than to \bar{r}_s . In this way the variation of the r -value, fig. 5, can be qualitatively explained.

5. Conclusions

1) The cold reduction, in case of the as cold-rolled sheets, cannot be considered as a factor to improve press-formability.

2) The drawability obtained with a flat-headed punch correlates well with the \bar{r} -value, which is best obtained for the 95% cold-rolled sheets in the partially recrystallized condition.

3) The drawability obtained with a round-headed punch and the stretchability correlate well with the n -value and the total natural strain respectively. They are best obtained with a fully recrystallized sheet.

4) The characteristic variation of r -value is qualitatively correlated with the texture obtained by means of pole figures. The development of both surface and mid-thickness layers with (112) $[11\bar{1}]$ and (123) $[21\bar{1}]$ textures is recommended for high r -values. These textures are the main textures that develop in both the surface and mid-thickness layers of the partially recrystallized sheet.

5) The higher \bar{r} -, \bar{n} -, and pure-stretch values for the 95% cold-rolled sheet and fully recrystallized, with respect to those for the 90% cold-rolled and fully recrystallized sheet, give an indication for the role of heavier reductions (higher than 95%) for improving the press-formability which is to be carefully examined.

6) Four ears are developed at the maximum r -value direction, r_{45} , independent of the cold-reduction and annealing temperature.

7) The variation of r -, n -, and Erichsen values of specimens annealed at various temperatures for one hour, have approximately the same value and tendency as those of specimens annealed for various temperatures at different annealing intervals.

6. References

- 1) Whiteley, R. L. et al., Sheet Metal Indust., Vol. 38, No. 409, 1961, p. 349.
- 2) Heyer, R. H. et al., Flat Rolled Products, III, 1962, p. 29, Interscience Publishers.
- 3) Matsudo, K. et al.*, J. Japan Soc. Technol. Plast., Vol. 8, No. 78 1967, p. 381.
- 4) Lankford, W. T. et al., Trans. ASM, Vol. 42, 1950, p. 1197.
- 5) Fukui, S. et al., Scientific papers of Inst. Phys. Chem. Res., Vol. 54, No. 2, 1960, p. 199.
- 6) Fukuda, M.*, J. Japan Soc. Technol. Plast., Vol. 5, No. 36, 1964, p. 3.
- 7) Yamada, Y.*, J. Japan Soc. Technol. Plast., Vol. 5, No. 38, 1964, p. 138.
- 8) Hosford, W. A. and Backofen, W. A., Fundamentals of Deformation Processing, 1964, p. 259, Syracuse University press.
- 9) Kawai, N. et al., Bull. of JSME, Vol. 12, No. 53, 1969, p. 1223.
- 10) Rogers, Jr., R. W. and Anderson, W. A., Metal Forming-Interrelation between theory and practice, 1971, p. 185, (AIME), Plenum press NY.
- 11) Riggs, B. A., Sheet Metal Indust., November 1973, p. 620.
- 12) Wright, J. C., Sheet Metal Indust., Vol. 39, No. 428, 1962, p. 887.
- 13) Gokyu, et al.*, J. Japan Inst. Metals, Vol. 30, No. 6, 1966, p. 591.
- 14) Oki, T. et al., Proceedings ICSTIS, Suppl. Trans. ISIJ, Vol. 11, 1971, p. 962, Tokyo.
- 15) Gokyu et al.*, J. Japan Inst. Metals, Vol. 30, No. 7, 1966, p. 669.
- 16) Grimes, R. et al., Sheet Metal Indust., Vol. 44, No. 482, 1967, p. 391.
- 17) Kawai et al., same reference as no. 9), p. 1232.
- 18) Schultz, L. G., J. Appl. Phys., 20, 1949, p. 1030.
- 19) Decker, B. F. et al., J. Appl. Phys., 19, 1948, p. 388.
- 20) Barret, C. S. and Masalski, T. B., Structure of Metals, 3rd edition, 1966, McGraw-Hill, Inc., NY.

- 21) Cullity, B. D., Elements of X-ray Diffraction, 1956, Addison-Wesely, Massachusetts.
- 22) Kemmis, O. H., Sheet Metal Indust., Vol. 34, March, 1957, p. 203.
- 23) Siebel, Stahl und Eisen, 74-3, 1954-1, p. 155.
- 24) Kawai, N. et al.**, The 20th meeting of the Japanese Society of Technology of Plasticity, Tokyo, November, 1966, p. 265.
- 25) Swift, H. W., Sheet Metal Indust., Vol. 31, No. 330, 1954, p. 817.
- 26) Kawai, N. et al., Bull. of JSME, Vol. 7, No. 28, 1964, p. 852.
- 27) Kawai, N. et al.*, J. Japan Soc. Technol. Plast., Vol. 8, No. 72, 1967, p. 28.
- 28) Kawai et. al.**, Trans. JSME, 40-338, 1974-10.
- 29) Recrystallization, Grain growth, and Textures-American Society of Metals, Ohio, 1966, p. 304.
- 30) Hsun, H. et al., J. of Metals, Jan. 1952, p. 76.
- 31) Hsun, H. et al., same reference as no. 30), p. 83.
- 32) Dillamore, I. L. et al., J. Inst. Metals, Vol. 92, 1963-64, p. 193.
- 33) Kamijo, T. et al.*, J. Japan Inst. Metals, Vol. 36, No. 1, 1972, p. 32.
- 34) Kamijo, T. et al.*, J. Japan Inst. Metals, Vol. 36, No. 7, 1972, p. 669.
- 35) Gokyu et al.*, J. Japan Inst. Metals, Vol. 29, No. 11, 1965, p. 1035.

* : in Japanese, synopsis in English.

** : in Japanese.